Gamma-ray spectroscopy for the characterization of uranium contamination in nuclear decommissioning

Francisco Salvador, Thomas Marchais, Bertrand Pérot, Pierre-Guy Allinei, Frédéric Morales, Olivier Gueton, Julien Venara, Marie Cuozzo, Frédéric Mayet

Gamma-ray spectroscopy for the characterization of uranium contamination in nuclear decommissioning

Francisco Salvador[1], Thomas Marchais[1], Bertrand Pérot[1], Pierre-Guy Allinei[1], Frédéric Morales[1], Olivier Gueton[2], Julien Venara[3], Marie Cuozzo[3], Frédéric Mayet[4]

[1]CEA, DES, IRESNE, DTN, SMTA, Nuclear Measurement Laboratory, F-13108 Saint-Paul-Lez-Durance, France
[2]CEA, DES, IRESNE, Nuclear Technology Department, 13108 Saint-Paul-lez-Durance, France
[3]CEA, DES, ISEC, DMPE, SEIP, LNPA, Univ. Montpellier, Marcoule, F-30207 Bagnols-sur-Cèze Cedex, France
[4]Laboratory of Subatomic Physics and Cosmology, CNRS/IN2P3, Grenoble Alpes University, 38026 Grenoble, France
Francisco.SALVADORBARBA@cea.fr

Abstract— Decommissioning is the last step in the life cycle of a nuclear facility. After the evacuation of the facility components, the remaining structures such as concrete walls and floors must be surveyed to ensure that no residual contamination remains. It is a costly and time consuming activity, for which CEA develops fast alpha and beta detection methods allowing a full scanning of very large areas (hundreds of thousands of square meters) in legacy uranium enrichment plants. To support these developments, we present here complementary high-resolution gamma-ray spectroscopy analyses of a contaminated area at the gaseous diffusion uranium enrichment facility UDG, currently under decommissioning at Pierrelatte nuclear plant, France. Long measurements are performed with a High-Purity Germanium (HPGe) detector on the contaminated surface, and in a clean area to assess the natural gamma background of the concrete ground. The surface activity of uranium is 16.6 ± 6.0 Bq.cm^{-2}, mainly due to ^{234}U and ^{238}U, most of the uncertainty coming from the non-uniform distribution of the contamination on the ground. This measurements also allowed us estimating the uranium enrichment of the contamination, which amounts to (0.80 ± 0.13) % of ^{235}U mass fraction, consistently with the range of the Low Enrichment Plant where this measure was performed. Eventually, the background spectrum allowed us to determine the mass fractions of natural uranium, thorium and potassium in the concrete ground, which respectively amount to 3.8 ± 0.2. ppm$_U$ (i.e. 3.8 mg of uranium per kg of concrete), 7.4 ± 0.7 ppm$_{Th}$, and (2.6 ± 0.1) %$_K$ of potassium.

Index Terms— HPGe detector, gamma-ray spectroscopy, MCNP simulation, uranium contamination, Decommissioning, Dismantling, UDG

I. Introduction

THE gaseous diffusion plant (UDG) of Pierrelatte nuclear site was the first uranium enrichment facility in France. It provided enriched uranium for both pressurised water reactors and for the development of nuclear weapons. The facility was operated from 1960 until its shutdown in 1996. Shortly after, the decommissioning operations began and the enrichment equipment has since been evacuated. As of today, a complete decommissioning of the UDG has yet to be approved by the nuclear safety authorities. Before the site is given clearance for decommissioning, a verification of the radiological cleanliness of the remaining concrete structures must be carried out to ensure the absence of residual uranium contamination. A full scan of UDG soils and walls, equivalent to 700 000 m^2, has to be performed to verify that the radioactivity level stay below a clearance alpha activity threshold of 0.4 Bq.cm^{-2}, established by the French Nuclear Safety Authority (ASN).

This calls for the development of fast measurement methods, capable of reaching low detection limits in very short acquisition times to measure large areas at a high rate. This can be achieved by alpha and beta contamination monitors, which are used as 1st level detectors, but when a contamination is detected, within a few seconds, a more precise quantification of the surface activity is needed as large interpretation uncertainties may occur due to the low range of alpha and beta particles in matter, especially in concrete. Therefore, the Nuclear Measurement Laboratory of IRESNE Institute, at CEA Cadarache, studies the use of gamma spectroscopy as an upper level quantification method of uranium contamination.

Gamma rays emitted by uranium contamination are mainly due to ^{238}U, ^{235}U and ^{234}U isotopes, and their direct descendants having a short enough half-life for radioactive equilibrium to be reached. Taking into account a decay period of 40 years as reference, corresponding to the UDG service life, the radioisotopes present in UDG contamination are thus ^{238}U, ^{234}Th, ^{234m}Pa, ^{235}U, ^{231}Th and ^{234}U. Their main gamma emissions (energy and intensity with their respective uncertainties) are presented in Table I.

TABLE I
MAIN GAMMA EMISSIONS FROM ISOTOPES PRESENT IN A URANIUM CONTAMINATION AFTER A 40 YEARS DECAY PERIOD [1]. AN ASTERISK (*) INDICATES THE STUDIED GAMMA RAYS.

Decay chain	Isotope	Gamma energy (keV)	Gamma intensity (%)
^{238}U	^{238}U	49.55 (6)	0.0697 (26)
	^{234}Th	63.30 (2) *	3.75 (8)
		92.38 (1)	2.18 (19)
		92.80 (2)	2.15 (19)
		112.81 (5) *	0.215 (22)
	^{234m}Pa	766.361 (20) *	0.323 (4)
		1 001.026 (18) *	0.847 (8)
^{235}U	^{235}U	143.767 (3) *	10.94 (6)
		163.356 (3) *	5.08 (3)
		185.720 (4) *	57.0 (3)
		205.316 (4) *	5.02 (3)
	^{231}Th	25.64 (2)	13.9 (7)
		84.2140 (13)	6.70 (7)
^{234}U	^{234}U	53.20 (2) *	0.1253 (40)

These gamma emissions compose the contamination signal and are predominantly present in the low energy region of the

gamma spectra, between 40 keV and 210 keV (see further Fig. 6). Only the gamma rays of ^{234m}Pa are outside this interval. During the uranium gaseous enrichment process, natural uranium is filtered in porous membranes to increase the proportion of ^{235}U and ^{234}U with respect to that of ^{238}U [2]. While the mass proportion of ^{234}U is very small, from about 0.005 to 0.006 % in natural uranium to 1 % in highly enriched uranium (HEU) [3], it brings more than 50 % of the alpha activity at low enrichment and up to almost 100 % for HEU, as a results of its short half-life of 245.10^3 years compared to 704.10^6 years for ^{235}U and 447.10^7 years for ^{238}U [1]. The UDG plant is made up of increasing enrichment facilities: the Low Enrichment Plant up to about 2 % (^{235}U mass fraction), the Medium Enrichment Plant (MP) up to about 8 % ^{235}U, the High Enrichment Plant (HP) up to about 25 %, and the Very High Enrichment Plant (VHP) up to more than 90 % [4]. Depending on the Enrichment Plant, the main contributors to alpha radioactivity significantly differ, as well as gamma emission rates.

Gamma detection is also subject to an important background emitted by the natural radioisotopes found in concrete, either in the natural decay chains of ^{238}U, ^{235}U, and ^{232}Th (uranium and thorium elements are present in concrete in ppm quantities, and their radioactive chains are in secular equilibrium), or by ^{40}K naturally present in potassium. Table II shows the most intense natural gamma emissions.

TABLE II
MAIN NATURAL GAMMA RAYS EMITTED IN CONCRETE, FROM ^{238}U, ^{235}U, ^{232}TH AND THEIR RADIOACTIVE DAUGHTERS, AND FROM ^{40}K [1]. A HASH (#) INDICATES THE STUDIED GAMMA RAYS.

Decay chain	Isotope	Gamma energy (keV)	Gamma intensity (%)
^{238}U	^{234}Th	63.30 (2)	3.75 (8)
		92.38 (1)	2.18 (19)
		92.80 (2)	2.15 (19)
	^{214}Pb	295.224 (2)	18.414 (36)
		351.932 (2) #	35.60 (7)
	^{214}Bi	609.312 (7) #	45.49 (19)
		1 120.287 (10) #	14.91 (3)
		1 238.111 (12)	5.831 (14)
		1 764.494 (14) #	15.31 (5)
^{232}Th	^{212}Pb	238.632 (2) #	43.6 (5)
	^{228}Ac	338.320 (5) #	11.4 (4)
		911.196 (6) #	26.2 (8)
		968.960 (9) #	15.9 (5)
	^{208}Tl	583.187 (2) #	30.6 (1)
		2 614.511 (10) #	35.84 (7)
	^{212}Bi	727.330 (9)	6.65 (4)
^{40}K	^{40}K	1 460.822 (6) #	10.55 (11)

We will show in next sections that this natural gamma background of concrete may represent a significant contribution in certain gamma rays, which must be subtracted to correctly estimate the activity of the uranium surface contamination. The measurement of this background and the detection of uranium contamination is reported in this work with a high resolution gamma spectroscopy detector, in the UDG Low Enrichment Plant.

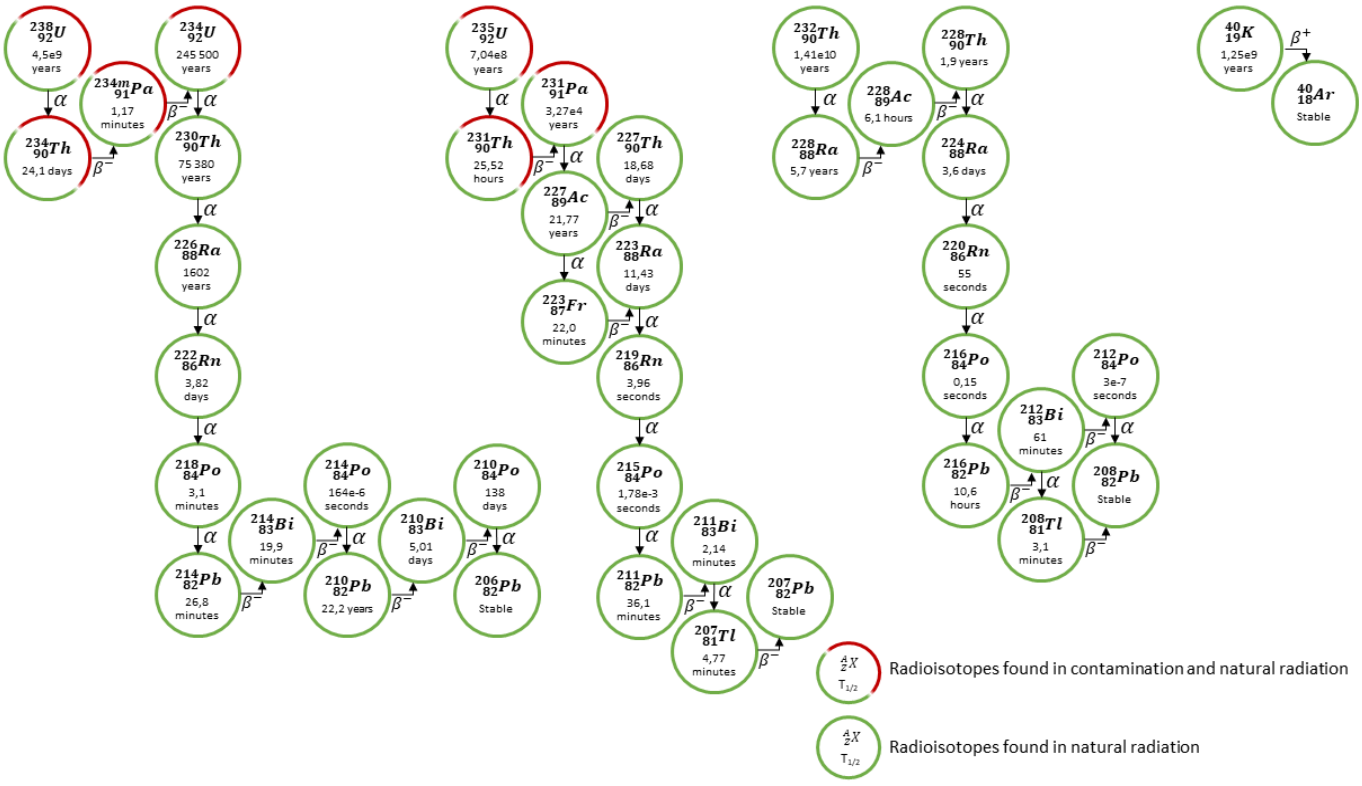

Fig. 1. ^{238}U, ^{235}U, ^{232}Th decay chains and ^{40}K decay. Decay data taken from [5].

II. High Resolution Gamma Spectroscopy for Fine Contamination Characterization

A. Measured areas

The measurements took place in a diffusion group of the UDG Low Enrichment Plant, especially on the reference area presented in Fig. 2, chosen because of the presence of a proven uranium contamination deposited over the concrete floor, which allows to compare different detection methods (alpha, beta, gamma).

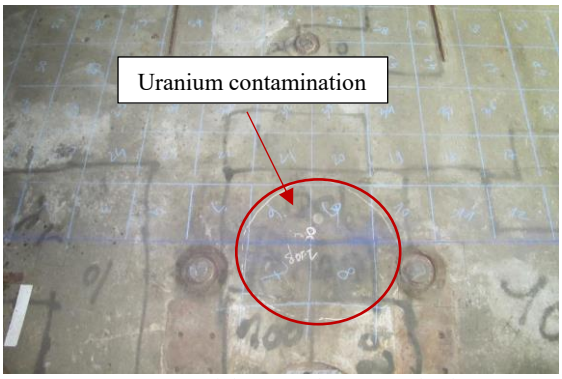

Fig. 2. Measurement area containing a uranium contamination spot.

The measurement area was separated into several measurement points (marked by the blue squares on Fig. 2) with an area of 25 cm × 25 cm each, which corresponds to the detection surface seen by our instruments. A label was attributed to each point and uranium contamination is located inside measurement points # 6, 7, 8 and 9. Other measurements were carried out on other points outside this region, which are supposed free of contamination, to estimate the concentration of natural gamma emitters in concrete (U, K, Th).

B. Experimental setup and MCNP model

High resolution gamma spectroscopy studies were conducted using a Falcon 5000 High Purity Germanium (HPGe) detector. This model includes a planar germanium crystal with a 6.5 cm diameter and 3 cm thickness, as well as an integrated multi-channel analyzer and an electrical cooling system [6]. Two measurement configurations were used, the first of which was used to measure uranium contaminated areas with the detector lifted 12.4 cm from the floor, thanks to a manual stacker (configuration # 1, see Fig. 3).

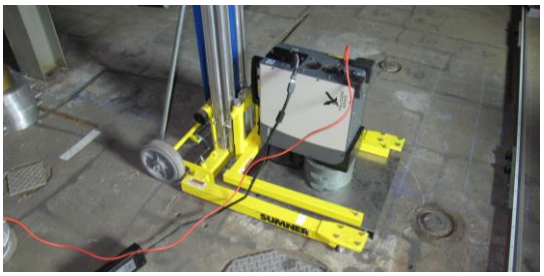

Fig. 3. Measurement setup # 1 with the HPGe detector for contamination measurement.

This setup led to a detection surface of 530 cm^2, similar to that of larger alpha and beta detectors used during the same measurement campaign, so that results could be compared. However, positioning the HPGe detector at this height above the ground reduces its detection efficiency. On the other hand, 5 cm thick lead rings were used to shield the germanium crystal against background radiation coming from neighboring soil surfaces but also from concrete walls.

In the second configuration, the HPGe detector is closer to the floor with a height of 6.7 cm between its entrance window and the ground (configuration # 2).

Fig. 4. Setup # 2 of the HPGe detector for background measurement.

This configuration # 2 allowed us to increase detection efficiency for the soil background measurements, while keeping the detector shielding. Monte-Carlo simulation models of both setups were developed with MCNP computer code [7] in order to calculate the detection efficiency of gamma rays emitted by uranium contamination, in surface, or by the bulk concrete soil for the natural background. These efficiencies are then used for activity calculations as detailed further in (1). The next figure shows a graphical representation of these MCNP models.

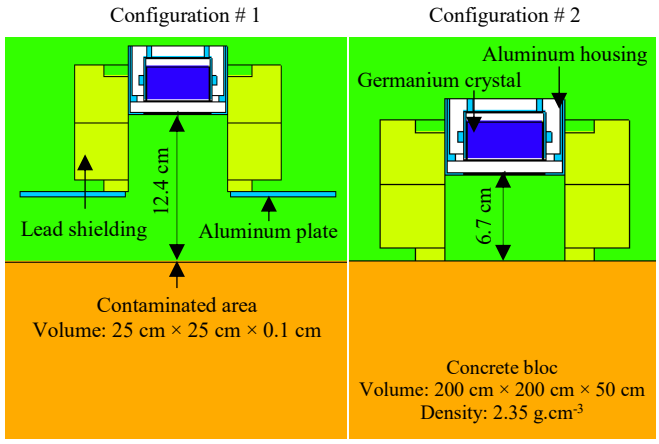

Fig. 5. Monte-Carlo models for germanium configurations # 1 and # 2 used for detection efficiency calculations.

For configuration # 1, the thin contaminated area (1 mm thickness) above the concrete ground is not visible in Fig. 5. It is also made of concrete and it is as a volume source in MCNP, while for configuration # 2, the source is the bulk concrete soil (50 cm thickness). The model of the detector and lead shielding is the same for both configurations.

C. Contamination activity estimation and enrichment percentage

As mentioned above, MCNP calculations are used to determine the gamma detection efficiencies allowing to convert the net measured count rates into activities (in Bq). Using detection setup # 1, an acquisition of 64.3 hours was performed on contaminated point # 7 located inside the contaminated area of Fig. 2. The obtained spectrum is given in Fig. 6.

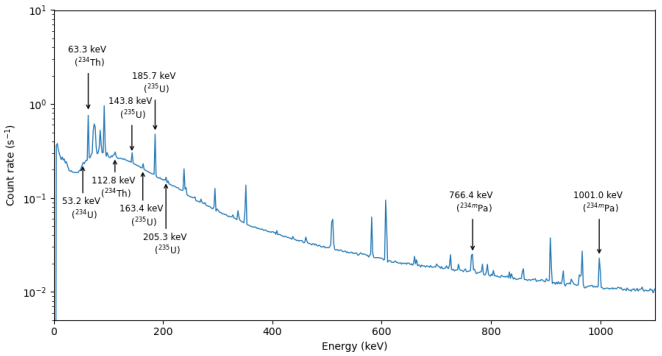

Fig. 6. Uranium contamination gamma spectrum measured in point # 7 with the HPGe detector. The main gamma peaks due to uranium contamination are indicated with arrows.

Uranium characteristic rays are visible on the spectrum, such as the 63.3 keV and 1001 keV lines emitted by ^{234}Th and ^{234m}Pa, respectively. Both isotopes are part of the ^{238}U contamination decay chain (see Table I). Peaks emitted by ^{235}U are also visible, for instance at 143.8 keV and 185.7 keV. A small 53.2 keV gamma from ^{234}U is also present (see Fig. 7).

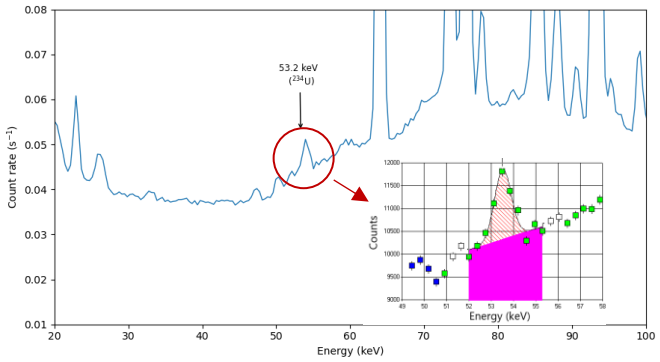

Fig. 7. Uranium contamination gamma spectrum measured in point # 7 with the HPGe detector zoomed between 20 and 100 keV to show the peak fit obtained with the Genie2000 gamma analysis software [8] for the 53.2 keV peak.

The activity of the emitting isotopes is estimated by analyzing gamma rays at different energies using the following equation:

$$A_S(E) = \frac{S_n(E)}{Eff(E) \times I(E) \times T_c \times S_{contamination}} \quad (1)$$

With:

- A_S the calculated surface activity (in Bq.cm^{-2}) calculated with peak of energy E (it is thus possible to calculate an average activity for the isotopes emitting several detectable gamma rays),
- $S_n(E)$ the net area under the gamma peak after subtraction of the Compton continuum under the peak, and of the net area of the natural background presented in Fig. 8 when it is significant, such as for the 185.7 keV peak of ^{235}U that is interfered by the 186.2 keV peak of ^{226}Ra in the background.
- Eff(E) the simulated detection efficiency (counts per source particle at energy E), calculated with the first model of Fig. 5. The migration depth of the uranium contamination was set to 1 mm to simulate a surface contamination. Other depth lengths from a few µm to a few mm were also considered but with a limited effect on simulated efficiency with a maximum relative difference of 4 % at low energy (53.2 keV),
- I(E) the emission intensity at energy E (number of gamma emitted per disintegration),
- T_c the active counting time (in seconds),
- $S_{contamination}$ the area of the contamination taken into account in the MCNP model, here 25 cm × 25 cm (see Fig. 5).

This led us to an estimation of the weighted average activity from the analysis of multiple gamma rays emitted by each of ^{238}U and ^{235}U isotopes. The average activities were calculated with the formula below:

$$\overline{A_x} = \frac{\sum_{i=1}^{N} \frac{A_s(E_i)}{\left(\frac{\sigma_{S_n}(E_i)}{S_n(E_i)}\right)^2}}{\sum_{i=1}^{N} \frac{1}{\left(\frac{\sigma_{S_n}(E_i)}{S_n(E_i)}\right)^2}} \quad (2)$$

With:

- $A_{s,i}$ the calculated surface activity from gamma peak at energy E_i (in Bq.cm^{-2}, refer to (1)) emitted by ^{238}U or ^{235}U,
- S_n the net area of the gamma peak at energy E_i
- σ_{Sn} the absolute statistical standard deviation for the gamma peak at energy E_i taking into account the background Compton continuum B under the peak, $\sigma_{Sn} = \sqrt{S_n + 2B}$ with S_n the net area and B the background.

From (2), we obtain the following weighted average activities: A_{238} = 8.4 ± 4.5 Bq.cm^{-2} and A_{235} = 0.44 ± 0.23 Bq.cm^{-2}. The estimation of ^{234}U activity relies on the only exploitable gamma peak at 53.2 keV, with an emission intensity of 0.13 %. Its net area fluctuates between 3711 and 5146 counts depending on fit parameters used to estimate the background under the peak (pink area in Fig. 7), with a relative standard deviation of 11 % and an average net area of 4090 counts resulting from 10 different fits. We added this standard deviation through a quadratic sum to the statistical standard deviation ($\sqrt{S_n + 2B}$), and thus estimate a total relative standard deviation of 17 % on the net area of the small 53.2 keV peak. Finally, we obtain the following activity for ^{234}U: A_{234} = 7.8 ± 4.1 Bq.cm^{-2}. We list below the different causes of uncertainty taken into account to estimate the previous confidence intervals on ^{234}U, ^{235}U, and ^{238}U activities:

- the representativeness of the MCNP model, especially the real distribution of the contamination, which was measured as non-uniform by autoradiography [9]. Therefore, we calculated efficiencies for multiple distribution hypothesis ranging from a hot spot (i.e. a point source in the middle of the collimator solid angle) to a surface of 30 cm × 30 cm exceeding the field of view of the detector inside the collimator (disk with a diameter of about 20 cm, i.e. a detection surface around 300 cm²). These calculations (not reported here) show that if the contaminated area is smaller (for instance a hot spot or a 10 cm × 10 cm surface) than the detector field of view, the efficiency can be almost

twice than that used for interpretation (calculated for a contaminated area of 25 cm × 25 cm) or those calculated with surfaces larger than the field of view (we studied from 20 cm × 20 cm to 30 cm × 30 cm). From this study and due to the lack of knowledge of the real contamination distribution, we consider an arbitrary relative uncertainty of 50 % on efficiency,

- this last also includes the uncertainty on the HPGe detector MCNP model, which is however less than 10 % from our feedback [10]. Even if this uncertainty is much smaller than the previous one, we will check the HPGe detector model through MCNP vs. experiment comparisons of precise measurements with calibration point sources, on the wide energy range of interest (53.2 keV peak of ^{234}U up to 1001 keV peak of ^{234m}Pa),
- the other uncertainties on the MCNP model, such as the limited knowledge of the concrete block density and chemical composition, are smaller and also included in the abovementioned 50 % relative standard deviation,
- statistical uncertainties, including the variability associated to the net area extraction for the small 53.2 keV peak of ^{234}U, and the dispersion of the activities obtained with the different peaks of multi-gamma emitters, calculated through the weighted average (2).

Summing the individual ^{238}U, ^{235}U and ^{234}U activity values, we obtain a total uranium activity of 16.6 ± 6.0 Bq.cm^{-2}.
HPGe measurements also allowed for an estimation of the enrichment percentage of the contamination. Individual activities of ^{238}U, ^{235}U, and ^{234}U are divided by their respective mass activities of 12.4×10^3 Bq.g^{-1}, 79.9×10^3 Bq.g^{-1} and 230×10^6 Bq.g^{-1} [1], to obtain the following masses m_{238} = 0.44 ± 0.05 g, m_{235} = (3.5 ± 0.4)×10^{-3} g and m_{234} = (2.1 ± 0.3) ×10^{-5} g. An ^{235}U enrichment of 0.80 ± 0.13 % is thus deduced using (3):

$$\%_{Enrichment} = \frac{m_{235}}{m_{235} + m_{238}} \times 100 \qquad (3)$$

This 0.8 % enrichment is consistent with the range of the Low Enrichment Plant, which extends from depleted uranium up to about 2 % [4], as mentioned in Section I. Since m_{235} and m_{238} are estimated from the measurement, only statistical uncertainties are considered but not those due to the possible non-uniformity of contamination.

D. Natural radiation measurements and U, K and Th concentration estimations

A 23 hour background measurement was done in a clean area using the HPGe detector in experimental configuration # 2 (see Fig. 4 and Fig. 5). The background spectrum is shown in Fig. 8, in which the well-known natural gamma rays are identified, such as the 609 keV peak of ^{214}Bi (bottom of ^{238}U decay chain), 1460 keV of ^{40}K, and 2614 keV of ^{208}Tl (end of ^{232}Th chain).

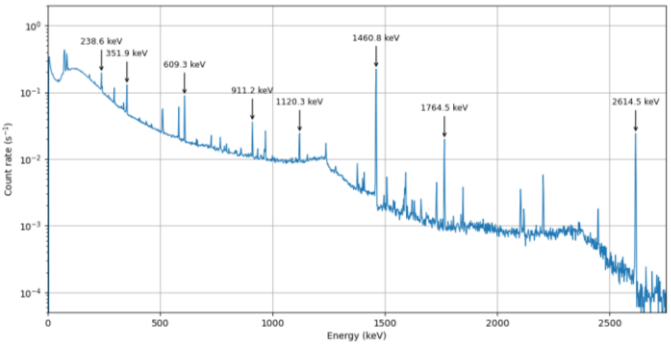

Fig. 8. Background spectrum measured with the HPGe detector with configuration # 2.

The efficiency is calculated with MCNP and the second model of Fig. 5 which considers a 200 cm × 200 cm × 50 cm concrete block of density 2.35 g.cm^{-3} as gamma source, which is a sufficient volume to have an almost infinite-equivalent geometry, i.e. no significant additional signal would come from a larger volume. We will investigate other geometries in future work, in particular to take into account new information about the real thickness of the ground at UDG Low Enrichment Plant. Note that this geometry leads to similar calculated activities for all gamma peaks (on a wide energy range) of the isotopes present in the ^{238}U and ^{232}Th natural chains, which are in secular equilibrium. The individual activities of each isotope is calculated as follows:

$$A_V = \frac{S_n(E)}{Eff(E) \times I(E) \times T_c} \qquad (4)$$

With:

- A_V the volume activity (in Bq) of ^{238}U or ^{232}Th calculated with the peak of energy E,
- $S_n(E)$ the net area under the gamma peak, after subtraction of the Compton continuum,
- Eff(E): simulated detection efficiency (counts per source particle at energy E), calculated with the second model of Fig. 5,
- I(E) and Tc as in (1).

Using (2), we obtain the following weighted average activities with the different peaks of ^{238}U and ^{232}Th chains: $A_{nat\ 238U}$ = 219 ± 14 kBq and $A_{nat\ 232Th}$ = 141 ± 14 kBq. On the other hand, the activity of ^{40}K estimated with the 1460 keV is $A_{nat\ 40K}$ = 3726 ± 192 kBq. The relative uncertainties are here ranging between about 5 and 10 %, which is much smaller than for contamination activity because natural U, Th and K elements are supposed uniformly distributed in the volume of concrete. The confidence intervals are therefore mainly due to counting statistics. The lack of knowledge of the real density and composition of the concrete ground has an effect smaller than 5 % on the energy range used to assess the above activities. From these activities, we can deduce the masses of U, Th and K elements present in the simulated concrete block, using the mass activities of the ^{238}U, ^{232}Th and ^{40}K isotopes (12.4 × 10^3, 4.07 × 10^3 and 265 × 10^3 in Bq.g^{-1} respectively, from [1]) and their natural abundance (99.3 % for ^{238}U, 99.9 % for ^{232}Th and 0.012 % for ^{40}K): m_U = 17.8 ± 1.1 g, m_{Th} = 34.6 ± 3.5 g and m_K = 120.4 ± 6.2 kg.

Taking into account the mass of the simulated concrete block, these masses corresponds to mass fractions of 3.8 ± 0.2 ppm_U for uranium (1 ppm is 1 mg of uranium per kg of concrete), 7.4 ± 0.7 ppm_{Th} for thorium and (2.6 ± 0.1) $\%_K$ for potassium. These mass fractions are within the range of typical U, K and Th proportions in the continental crust [11].

III. Conclusion

Experimental tests have been performed at the UDG uranium gaseous enrichment plant for the detection of residual uranium contamination, using high resolution gamma spectroscopy with an HPGe detector. This measurement of 64 hours allowed us to evaluate the surface activity of a contaminated area to 16.6 ± 6.1 $Bq.cm^{-2}$. The large uncertainty is mainly due to the limited knowledge of the real contamination distribution, which has been demonstrated to be non-homogenous thanks to autoradiography analysis [9]. We also measured the ^{235}U mass enrichment, estimated to (0.80 ± 0.13) %, and the natural background over a clean area of the facility. From the study of this background spectrum, we evaluated the natural U, Th and K mass fractions to 3.8 ± 0.2 ppm_U, 7.4 ± 0.7 ppm_{Th} and (2.6 ± 0.1) $\%_K$ inside the facility concrete, which is consistent with typical continental crust levels [11]. Future works will focus on low resolution gamma spectroscopy with an NaI(Tl) scintillator on the same contaminated area. The goal being to have a faster characterization (about 15 min) of the contaminated surfaces detected by alpha or beta contamination monitors.

References

[1] M.-M. Bé, V. Christé, and C. Dulieu, "NUCLÉIDE-LARA - Bibliothèque des émissions alpha, X et gamma," *Rapp. CEA R-6201*.

[2] W. Jeff, "Uranium conversion and enrichment," in *Nuclear Fuel Cycle Science and Engineering*, Elsevier, 2012, pp. 151–176. doi: 10.1533/9780857096388.2.151.

[3] S. Croft *et al.*, "The specific (α ,n) production rate for 234 U in UF 6," *Nucl. Instrum. Methods Phys. Res. Sect. Accel. Spectrometers Detect. Assoc. Equip.*, vol. 954, p. 161608, Feb. 2020, doi: 10.1016/j.nima.2018.11.067.

[4] S. Philippe and A. Glaser, "Nuclear Archaeology for Gaseous Diffusion Enrichment Plants," *Sci. Glob. Secur.*, vol. 22, no. 1, pp. 27–49, Jan. 2014, doi: 10.1080/08929882.2014.871881.

[5] J. Peterson, M. MacDonell, L. Haroun, and F. Monette, "Radiological and Chemical Fact Sheets to Support Health Risk Analyses for Contaminated Areas," Argonne National Laboratory, Environmental Science Division, Mar. 2007.

[6] Mirion Technologies, "Falcon 5000® Portable HPGe-Based Radionuclide Identifier." Accessed: Jul. 26, 2022. [Online]. Available: https://mirion.s3.amazonaws.com/cms4_mirion/files/pdf/spec-sheets/falcon-portable-hpge-based-identifier.pdf?1557257239

[7] J. Kulesza *et al.*, "MCNP® Code Version 6.3.0 Theory & User Manual," LA-UR-22-30006, 1889957, Sep. 2022. doi: 10.2172/1889957.

[8] Mirion Technologies, "GENIE™ 2000 Gamma Analysis Software."

[9] P. Fichet, S. Leblond, R. Laumonier, P. Sardini, and S. Billon, "MAUD Project - Characterization by Autoradiography Tech-nique of facilities under dismantlement," 2018.

[10] T. Marchais *et al.*, "Detailed MCNP Simulations of Gamma-Ray Spectroscopy Measurements With Calibration Blocks for Uranium Mining Applications," *IEEE Trans. Nucl. Sci.*, vol. 65, no. 9, pp. 2533–2538, Sep. 2018, doi: 10.1109/TNS.2018.2797312.

[11] K. S. Heier, "Radioactive Elements in the Continental Crust," *Nature*, vol. 208, no. 5009, pp. 479–480, Oct. 1965, doi: 10.1038/208479b0.